

## *Isotope Effect in Bilayer WSe<sub>2</sub>*

Wei Wu<sup>1,2</sup>, Mayra Daniela Morales-Acosta<sup>2</sup>, Yongqiang Wang,<sup>3,4</sup> Michael Thompson Pettes<sup>1,2,4,\*</sup>

<sup>1</sup>Department of Mechanical Engineering, University of Connecticut, Storrs, Connecticut 06269, United States

<sup>2</sup>Institute of Materials Science, University of Connecticut, Storrs, Connecticut 06269, United States

<sup>3</sup>Materials Science and Technology Division, Los Alamos National Laboratory, Los Alamos, New Mexico 87545, United States

<sup>4</sup>Center for Integrated Nanotechnologies (CINT), Materials Physics and Applications Division, Los Alamos National Laboratory, Los Alamos, New Mexico 87545, United States

\*Corresponding Author, E-mail: [pettesmt@lanl.gov](mailto:pettesmt@lanl.gov).

### 1. Growth of single crystal naturally abundant <sup>NA</sup>W<sup>NA</sup>Se<sub>2</sub> and isotopically pure <sup>186</sup>W<sup>80</sup>Se<sub>2</sub> bilayers

Naturally abundant <sup>NA</sup>W<sup>NA</sup>Se<sub>2</sub> and isotopically pure <sup>186</sup>W<sup>80</sup>Se<sub>2</sub> bilayers were grown by a chemical vapor deposition (CVD) method<sup>1</sup>. 200 mg of <sup>NA</sup>WO<sub>3</sub> powder (Sigma-Aldrich, 99.9% purity) or <sup>186</sup>WO<sub>3</sub> (ISOFLEX USA, >99.90% purity) in a crucible was placed in the center of furnace equipped with a 1-inch diameter quartz tube. 200 mg of <sup>NA</sup>Se powder (Alfa Aesar, 99.999% purity) or <sup>80</sup>Se powder (ISOFLEX USA, >99.90% purity) was loaded into a separate crucible placed upstream at the edge of the furnace heating zone. Tungsten diselenide crystals were grown on a single-side-polished SiO<sub>2</sub> (~285 nm thickness)/Si substrate placed polished-side-down on top

of the crucible containing the  $^{186}\text{W}^{18}\text{O}_3$  or  $^{186}\text{W}^{18}\text{O}_3$  powder. The CVD reactor was first pumped to lower than  $10^{-4}$  mbar by a mechanical pump, followed by injection of gaseous  $\text{H}_2$  (4.992%)/ $\text{N}_2$ (balance) (Airgas, 99.999% purity) at  $100\text{ cm}^3\text{min}^{-1}$ . Once the pressure in the growth chamber was raised to atmospheric pressure, the exhaust of CVD system was switched to a sealed bubbler filled with silicone oil (Sigma-Aldrich) in order to maintain atmospheric pressure and prevent air from diffusing back into the system. The flow rate of  $\text{H}_2/\text{N}_2$  was then reduced to  $50\text{ cm}^3\text{min}^{-1}$  for the growth. The furnace temperature during growth was set at  $1000^\circ\text{C}$ , while the Se temperature was measured to be  $\sim 290^\circ\text{C}$ . By adjusting the position of Se crucible, we optimized the time at which Se vapor was introduced in order to grow the bilayer tungsten diselenide single crystals with uniform thickness. High yield growth was achieved by melting the Se powder when the center of the furnace reached  $\sim 820^\circ\text{C}$ . After the growth, the reactor was cooled to  $750^\circ\text{C}$  in 20 minutes; and then rapidly cooled to room temperature by opening the furnace lid. Atomic force microscopy analysis of  $^{186}\text{W}^{80}\text{Se}_2$  bilayer crystallites showed uniform thicknesses of  $\sim 1.3\text{ nm}$ , in accordance with the out-of-plane unit cell parameter of bulk tungsten diselenide, which is  $12.9825\text{ \AA}$  (powder diffraction file no. 38-1388)<sup>2</sup>. The growth resulted in crystal sizes on the order of  $5\text{--}15\text{ }\mu\text{m}$ .

## 2. X-ray diffraction (XRD) characterization

A Bruker D5005 X-ray diffractometer with Cu  $K_{\alpha}$  radiation ( $\lambda = 1.54184 \text{ \AA}$ ) operated at 40 kV and 40 mA was used to perform X-ray diffraction (XRD) measurements at room temperature. XRD analysis for  $d$ -spacing and crystallite size was performed by peak profile fitting with a pseudo-Voigt function using MDI Jade software. Figure S1 gives the XRD patterns of  $^{NA}W^{NA}Se_2$  and  $^{186}W^{80}Se_2$  with both linear and logarithmic ordinate axis.

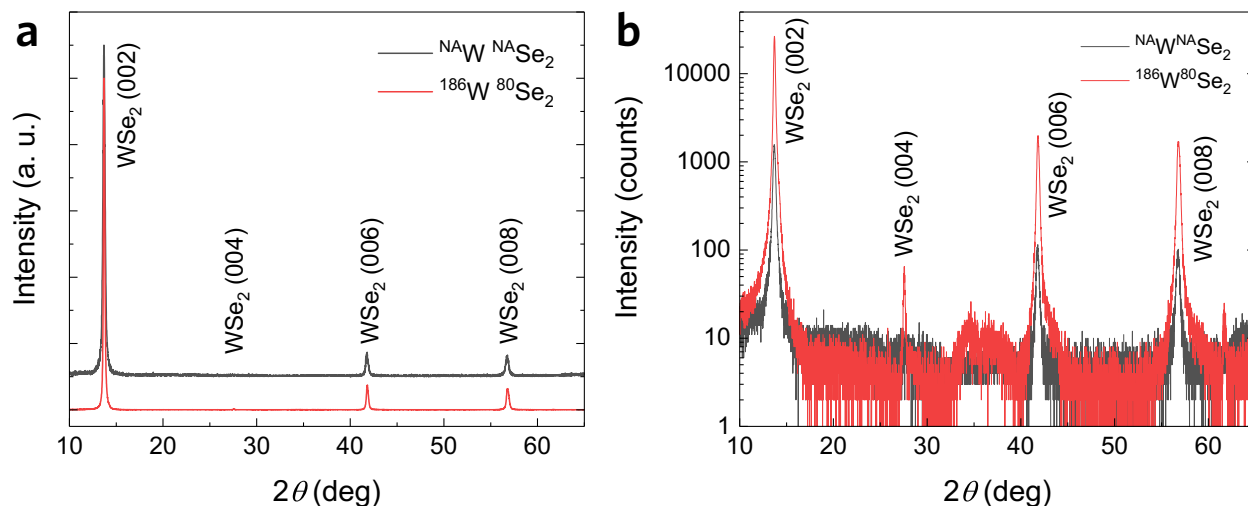


**Figure S1.** (a) Linear-linear and (b) log-linear XRD patterns of naturally abundant  $^{NA}W^{NA}Se_2$  (black line) and isotopically pure  $^{186}W^{80}Se_2$  (red line). The diffractograms are aligned to the Si (004) peak to correct for specimen displacement.

Since the length of the sample irradiated by the X-ray beam is on the order of a millimeter, the signal is collected from an ensemble average of deposited materials and allows for unit cell parameter refinements to be performed. The Si (004) peak position of the substrate at  $2\theta = 69.173^\circ$  (powder diffraction file no. 05-0565) was employed as reference to correct for specimen

displacement. The XRD analysis for  $d$ -spacing and crystallite size was performed by peak profile fitting with a pseudo-Voigt function using MDI Jade software. The diffractograms of the thin films were referenced to a hexagonal phase of  $\text{WSe}_2$  (P63/mmc, space group 194, powder diffraction file no. 38-1388)<sup>2</sup>. Besides the expected Si (004) peak, the XRD patterns displayed four distinct characteristic peaks assigned to the (002), (004), (006) and (008) crystal planes of  $\text{WSe}_2$ , indicating the thin films are all oriented along the  $c$ -axis. The interlayer spacing determined from the (002) peak is  $6.4670 \pm 0.0032 \text{ \AA}$  and the  $c$ -lattice parameter is  $12.9341 \pm 0.0067 \text{ \AA}$  for the  $^{187}\text{W}^{187}\text{Se}_2$  samples, whereas the (002) interlayer spacing and the  $c$ -lattice parameter are  $6.4646 \pm 0.0007 \text{ \AA}$  and  $12.9298 \pm 0.0024 \text{ \AA}$  for  $^{186}\text{W}^{80}\text{Se}_2$  samples. The  $c$ -lattice parameter difference between  $^{187}\text{W}^{187}\text{Se}_2$  and  $^{186}\text{W}^{80}\text{Se}_2$  is 0.033 % which is on the order of the difference observed between  $h$ - $^{10}\text{BN}$  and  $h$ - $^{11}\text{BN}$  (0.035%)<sup>3</sup>, where the XRD instrumental uncertainty after peak profile fitting in this work is on the order of 0.02–0.05 %. Heavier atomic mass isotopes tend to exhibit smaller van der Waals radii; the van der Waals radius of deuterium ( $^2\text{H}$ ) is  $\sim 1.15 \text{ \AA}$ , whereas that of hydrogen ( $^1\text{H}$ ) is  $\sim 1.20 \text{ \AA}$ <sup>4</sup>. By calculating the ratio of relative van der Waals radius change to relative change in atomic mass, we note that the small difference we observe in the  $c$ -axis unit cell parameter for  $\text{WSe}_2$  (-0.027) actually corresponds well to that expected for hydrogen (-0.042). Although it is hard to draw a further quantitative conclusion of the isotopic effect on lattice parameters due to the instrumental uncertainty, the subsequent analysis indicates that such small lattice parameter changes are expected to have a negligible effect on the phonon dispersion and optical band gap in comparison to the isotope effect.

### 3. Mass spectrometry of WSe<sub>2</sub>

Rutherford backscattering spectrometry (RBS) was conducted on a National Electrostatics Corporation 3 MV Tandem Accelerator using a 2 MeV <sup>4</sup>He<sup>+</sup> ion beam. A solid-state silicon detector located at 167° from the beam direction was used to detect the scattered He particles. Comparison of the W and Se peak areas yields the atomic ratio through the expression

$$c_{\text{Se}}/c_{\text{W}}=(A_{\text{Se}}/A_{\text{W}})/(\sigma_{\text{W}}/\sigma_{\text{Se}}), \quad (\text{S1})$$

where  $c$  is the atomic areal density,  $A$  is the peak integrated area, and  $\sigma$  is the Rutherford scattering cross section. The RBS method in theory can have very high accuracy of determining atomic ratios (1-2%), however the peak area determination for each element could introduce 5-10% error as a result of signal pileups from substrate scattering and signal overlaps between similar mass elements in measurements.

Analyzing the mass ratios according to WSe<sub>2-x</sub>, we obtain sub-stoichiometry parameters of  $x = 0.021$  for the naturally abundant sample and  $x = 0.023$  for the isotopically enriched sample which are both within the experimental uncertainty indicating comparable stoichiometry and sample quality.

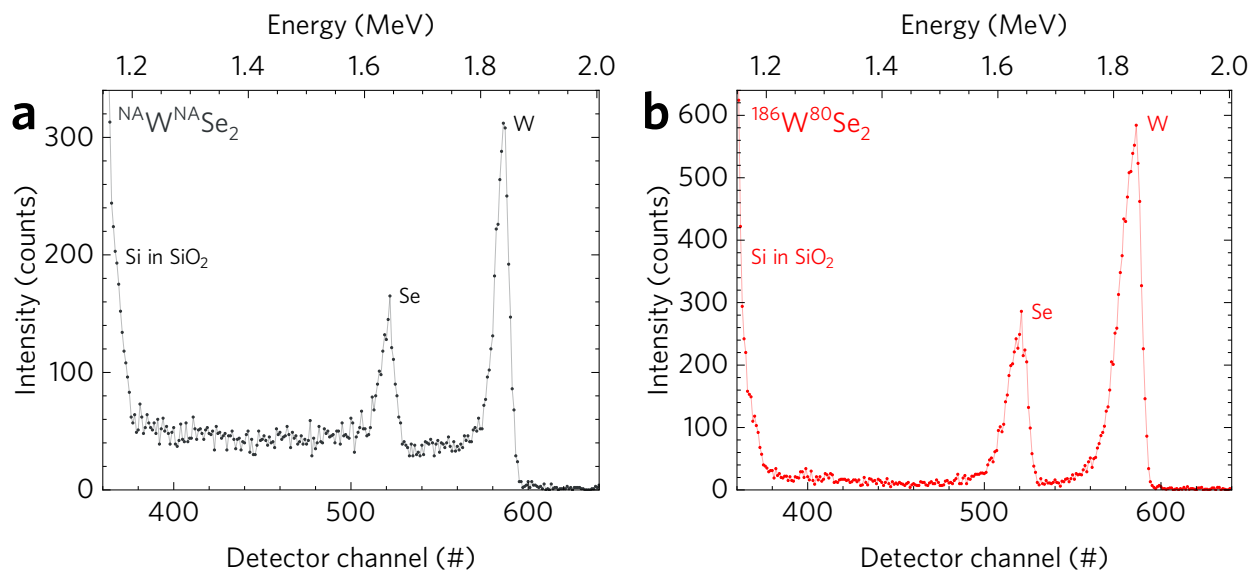


**Figure S2.** RBS spectra for (a)  ${}^{\text{NA}}\text{W}^{\text{NA}}\text{Se}_2$  and (b)  ${}^{186}\text{W}{}^{80}\text{Se}_2$ . Comparison of W and Se peak areas yields stoichiometry, and signal to noise is sufficient to determine stoichiometry after background subtraction.

#### 4. Raman and photoluminescence spectroscopy

Raman and photoluminescence spectroscopy were conducted on a Horiba LabRAM HR Evolution system. The spatially dependent room-temperature spectra were obtained using 2.33 eV ( $\lambda=532$  nm) continuous wave laser excitation with a beam diameter on the order of 250 nm and total power of 86  $\mu$ W measured by a THORLABS PM100D power meter. Power was kept below 100  $\mu$ W to avoid sample damage or spectra shifts due to local heating effects. The integration time was 1 s and 2 s for spatially dependent Raman and photoluminescence maps, respectively. The gratings used were 1800 grooves/mm for Raman, and 600 grooves/mm for photoluminescence.

For temperature dependent Raman and photoluminescence analysis, both  $^{NA}W^{NA}Se_2$  and  $^{186}W^{80}Se_2$  samples on Si/SiO<sub>2</sub> were mounted into a Janis Research Company ST-500 optical cryostat while a continuous liquid helium flow was supplied. Before cooling, the sample chamber was pumped to lower than  $10^{-6}$  mbar. The sample mount temperature was controlled by a Lakeshore 335 temperature controller. The system was stabilized at each set-point temperature for at least 1 hour before characterization. To avoid non-uniform temperature distribution within or between samples, all the Raman spectra were aligned using the silicon peak at each temperature. The integration time was 4 s for Raman and 6 s for photoluminescence spectroscopy, respectively. The gratings used were 1800 grooves/mm for Raman, and 600 grooves/mm for photoluminescence. The PL spectra showing power normalized absolute emission intensity is plotted in Figure S3.

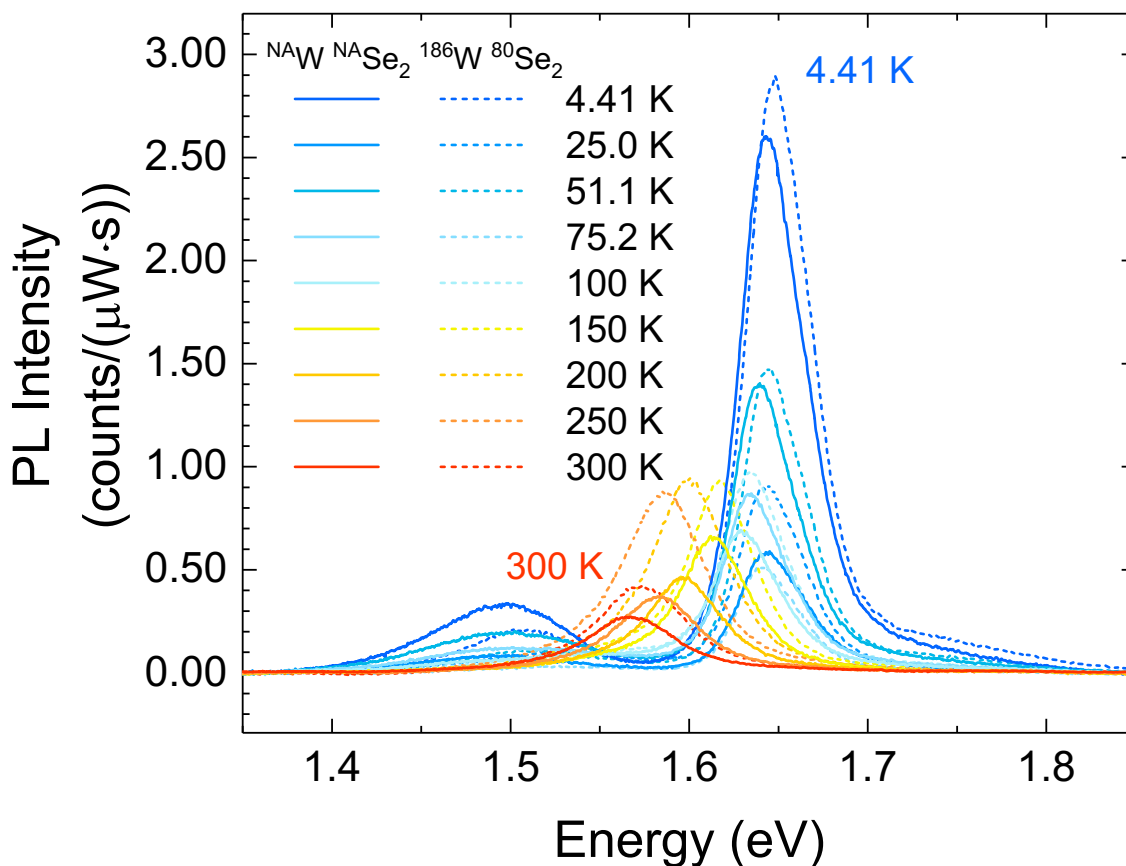


**Figure S3.** Photoluminescence spectra of bilayer  $^{NA}W^{NA}Se_2$  (solid lines) and isotopically pure bilayer  $^{186}W^{80}Se_2$  (dashed lines).

### Supporting References

- (1) Wu, W.; Wang, J.; Ercius, P.; Wright, N. C.; Leppert-Simenauer, D. M.; Burke, R. A.; Dubey, M.; Dongare, A. M.; Pettes, M. T. Giant mechano-optoelectronic effect in an atomically thin semiconductor, *Nano Lett.* **2018**, *18*, 2351–2357.
- (2) Wong-Ng, W.; McMurdie, H. F.; Paretzkin, B.; Zhang, Y.; Davis, K. L.; Hubbard, C. R.; Drago, A. L.; Stewart, J. M. Reference x-ray diffraction powder patterns of fifteen ceramic phases, *Powder Diffr.* **1987**, *2*, 257–265.
- (3) Vuong, T. Q. P.; Liu, S.; Van der Lee, A.; Cuscó, R.; Artús, L.; Michel, T.; Valvin, P.; Edgar, J. H.; Cassabois, G.; Gil, B. Isotope engineering of van der Waals interactions in hexagonal boron nitride, *Nat. Mater.* **2017**, *17*, 152–158.
- (4) Libby, W. F. Isotope size effect in van der Waals radii and the barrier to rotation around the carbon-carbon single bond, *J. Chem. Phys.* **1961**, *35*, 1527–1527.